

PARAMETRIC ANALYSIS OF COMPOSITE REINFORCED WOOD TUBES UNDER AXIAL COMPRESSION

Jose M. Cabrero¹, Andreas Heiduschke², Peer Haller³

ABSTRACT: Wood tubes combine economy, an efficient use of the material and optimal structural performance. They can be optionally reinforced with technical fibers and/or textiles laminated to the outer wood surface. The paper presents the outcomes of a parametric study on the performance of wood reinforced tubes submitted to axial compression. Simple analytical models were applied to estimate the load-carrying capacity of the tubes and their failure mechanisms. Analytical and numerical models were developed to simulate and analyze the load-carrying behavior of the tubes and their failure mechanisms as well as to determine the required lay-up of the reinforcement. Developed analytical models are based on the Classical Laminate Theory in combination of the Tsai-Wu failure criteria. The models were calibrated and verified through the experimental data to assess their reliability. Predicted and experimental failure mechanisms and loads agreed reasonably well. Herein, several parametrical analyses based on the analytical model are presented. However, in the future, more sophisticated analytical models have to be developed and further tests on tubes with varying r/t and l/r ratios are required to verify these models.

KEYWORDS: Efficiency, FRP, Analytical models, Axial strength, Tsai-Wu failure criteria, Optimization, Design

1 INTRODUCTION

Our design objectives are increasingly determined by the need of a sustainable economical development. Thus, an efficient use of the available materials becomes increasingly important. Apart from the material properties, the structural and economical performance of the cross section is the most important design issue.

Structural elements must safely transfer forces and moments and simultaneously meet the serviceability requirements. The moment of inertia of the section is a major parameter for both required tasks. However, in the case of timber, by means of the traditional transformation technologies (sawing. . .), round or square solid cross sections are produced. These traditional cross sections are less competitive and efficient when compared to more engineered sections, such as steel profiles.

From those thoughts, a procedure of manufacturing wooden profiles has been developed and patented [1]. Wood is compressed in its transverse direction up to 50% of its original size by folding its microstructure. This is a reversible process and the principle of this innovative process, where thick solid panels of compressed wood are transformed to open or closed prismatic cross sections (Figure 1).

This manufacturing principle may be applied to a wide variety of sections: all open and closed prismatic cross-sections may be produced in a continuous manufacturing process. The resulting profile encompasses efficient use of the material and optimal structural performance. The here proposed and analysed circular hollow sections behave well when subjected to axial forces, so they are well suited for columns.

Depending on the wall thickness of the timber profile, an additional fibre reinforced plastic (FRP) glued to the outer surface of the profile might be required to strengthen the wood [1]. Thin walled profiles are prone as well to develop longitudinal cracks due to shear and tensile stresses perpendicular to the grain.

Load adapted FRP reinforcement can avoid brittle type failures of the profiles. Both materials benefit: wood profits from the outstanding mechanical and physical characteristics of FRP, while FRP does it from the mechanical characteristics and the low price of wood as well as its environmental friendliness. Wood profiles are well suited for the use in light-weight structures, the classical field of FRP composites. The use as a permanent winding core can help to reduce manufacturing costs. The wooden core will eliminate

¹ Jose M. Cabrero. Department of Structural Analysis and Design, School of Architecture, University of Navarra. 31080 Pamplona, Spain. Email: jcabrero@unav.es, web: <http://www.unav.es/estructuras/>

² Andreas Heiduschke, Institut für Stahl- und Holzbau, Technische Universität Dresden, 01062 Dresden, Germany Email: andreas.heiduschke@tu-dresden.de, web: <http://www.tu-dresden.de/biwibh/g>

³ Peer Haller, Institut für Stahl- und Holzbau, Technische Universität Dresden, 01062 Dresden, Germany Email: peer.haller@tu-dresden.de, web: <http://www.tu-dresden.de/biwibh/>

local buckling effects and strengthen the FRP profile in axial direction.

The presented research work deals with the development of an analytical model to obtain the axial strength for the design of the wooden tubes reinforced with glass-fibre-epoxy composite subjected to simple axial compression loading.

The model results are compared to the available experimental results [2,3], which are presented in this conference as well [4]. In this paper, the accomplished parametrical analyses are explained.

2 DEVELOPED ANALYTICAL MODEL

A brief explanation of the developed analytical model is given here. Further explanations may be found in [5] or [6].

Figure 2 depicts the algorithm in a graphical way. In the strain space, the Tsai-Wu failure criteria of the layers of a composite material is plotted. Strain space must be used, since both layers (in a thin shell theory) share the strain when submitted to axial loading. And also, the failure envelope of the layer is an invariant in the strain space. Given a state of strain, it may be easily plotted into the graph as point *A*, where both coordinates are known.

It is assumed that for this strain state, the corresponding stress state is known, and given in a stress vector.

If assumed as well that the initial unloaded strain state of the laminate corresponded to zero strains, namely, no residual stresses were present. Since the laminate is room temperature cured, it seems reasonable in this particular application (if initial or residual stresses were present, the applied vectors would radiate from a point different to the origin). Therefore, the corresponding strain response line *B* up to the actual strain state; (depicted with point *A*) may be plotted.

Proportional loading is assumed, so this response line *B* may be extended until its intersection with the failure criteria envelope in point *C*. The intersection would correspond to the failure strain state of the laminate (First Ply Failure is assumed). The corresponding state of combined stresses for the failure strain state may be obtained.

The proportional loading assumption allows to obtain an additional intersection point with the failure envelope, *T*. The corresponding stress vector for the failure strain corresponds to the failure stress state of opposite sign to *C*. In the case of uniaxial longitudinal loading, i.e. point *C* would represent the failure for a compressive loading, while *T* the failure for a tensile loading.

2.1 APPLICATION TO THE EXPERIMENTAL RESULTS

The analytical model presented in the previous Section is applied to the experimental results (Figure 3).

The mean error is less than 3%, with a standard deviation of the predictions less than 5%. A good correlation is thus observed with the experiments of about 2.5m height. Several parametrical analyses may be accomplished with it to obtain a more comprehensive understanding of the tubes.

3 PARAMETRICAL ANALYSES

3.1 INFLUENCE OF THE FIBER ORIENTATION

As explained in the previous Sect.2, the analytical model derived allows to obtain both the failure for simple compression or tension loading. Figure 4 shows the predicted failure stresses for a composite with 19mm thick wood wall plus a 1mm cross-ply fiber reinforcement.



Figure 1. Wooden formed tube

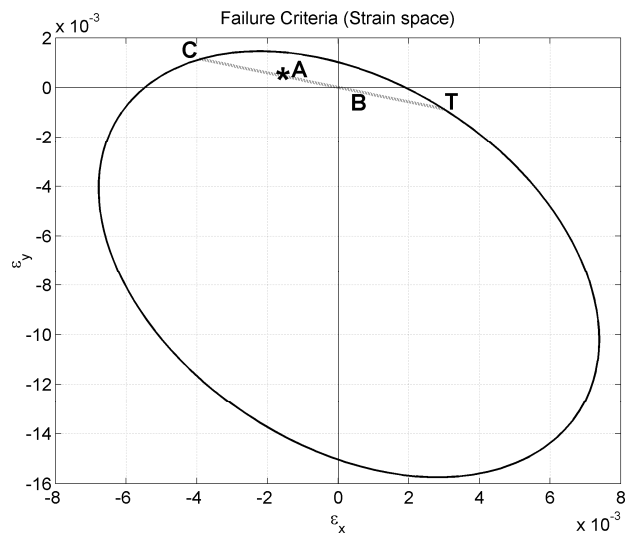


Figure 2. Graphical application of the analytical model

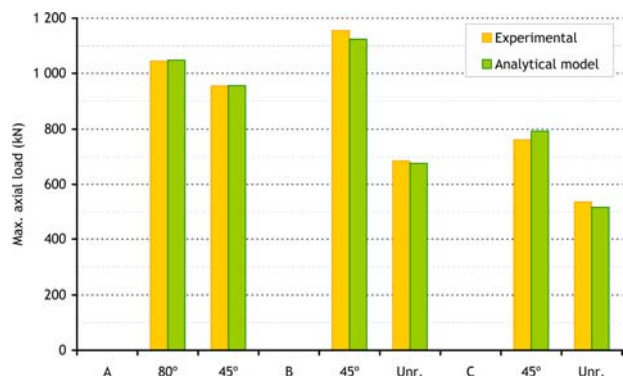


Figure 3. Comparison of the analytical and experimental results

The maximum failure stress for a compressive force is achieved for a fiber reinforcement $\pm 0^\circ$, 62.74 N/mm^2 . The failure stress has another local maximum for a fiber orientation of $\pm 90^\circ$ (reinforcement perpendicular to the longitudinal direction of the wood), just 1.5% lower. The minimum failure stress is among the interval between $\pm 40^\circ$ and $\pm 45^\circ$, about 9% lower (57 N/mm^2 approximately). These predictions confirm the trend already observed in the experimental tests: a perpendicular reinforcement provides a better response. In the case of the tension failure stress, values are about 20 N/mm^2 less in comparison to the compression case. The maximum strength is obtained for a fiber reinforcement of $\pm 25^\circ$, 43.63 N/mm^2 . Quite similar values are obtained for reinforcements ranging from $\pm 0^\circ$ up to this orientation. From this angle, the failure stress decreases, up to a value 10% less when the fiber reinforcement is $\pm 90^\circ$.

From these figures, it may be derived that a single cross-ply reinforcement, with good performance for both tension and compression loadings is achieved with a cross-ply reinforcement closer to $\pm 0^\circ$.

3.2 BUCKLING OF THE WOODEN REINFORCED TUBES

The analytical buckling equations for composite tubes described in [7] are applied to the wooden reinforced tubes. The analysed tubes correspond to those from the experimental series: wood 19mm, cross-ply fiber 1mm thick, 2.5m high.

It may be seen in the resulting graphs (Figure 5) how the local buckling modes do not influence their behaviour. The global Euler mode arises always for lower loads. Almost no influence of the fiber reinforcement on the global buckling is appreciated (as also shown in Fig. 5). A clear influence of the fiber reinforcement may be observed for the local buckling modes. The ring buckling mode is produced for higher loads the more perpendicular the reinforcement. For the chessboard buckling, the higher loads are obtained for reinforcements in the range from $\pm 45^\circ$ to $\pm 90^\circ$ (resulting in an almost constant load for the analysed range).

3.3 THREE-DIMENSIONAL DESIGN GRAPH

A number of plots to understand the new material formed by the wood and the fiber reinforcement may be done. A three-dimensional graph accounting for the failure compression stress in relation to the thickness of the wood layer and the radius of the tube is shown in Figure 6. This figure is done as a demonstration, for a $\pm 85^\circ$ glass-fibre-epoxy fiber reinforcement 1mm thick. The shown graph intends to be a kind of a design graph. Apart from the material's failure stress derived by means of the analytical model (Sect. 2), the buckling stresses corresponding to the different buckling modes (Sect. 3.2) are depicted. The surfaces corresponding to the Euler's buckling for different lengths of the tube are drawn, as well as the two different local buckling modes, ring and chessboard buckling.

The Euler buckling stress depends to a great extent on the column length. It also depends to a great extent from the radius of the tube, and to a lesser extent from the

thickness of the wall. This result is related to the moment of inertia of the section, which depends mainly on the radius.

For the analysed tube, ring buckling does not occur. Its values are always higher than those of the material strength.

The chessboard buckling may occur, but only for tube radius over 300mm, with layer thicknesses lower than about 12mm. The range where it happens is very restricted.

It applies to thin layers where Euler buckling is already prevented due to their high moment of inertia.

The material strength is independent from the radius of the tube. In fact, this variable is not taken into account in the analytical model. It also seems almost independent from the thickness of the wood layer. The corresponding contour is almost a plane, with a little higher value the thicker the wood.

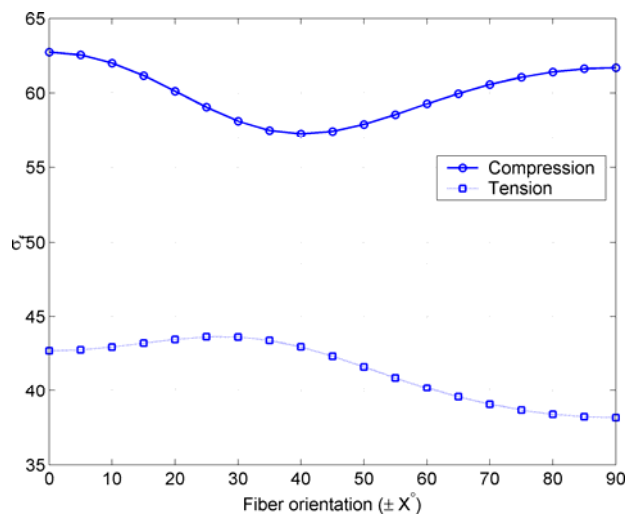


Figure 4. Failure stress variation according to fiber reinforcement orientation. Wood 19mm, cross-ply fiber 1mm thick.

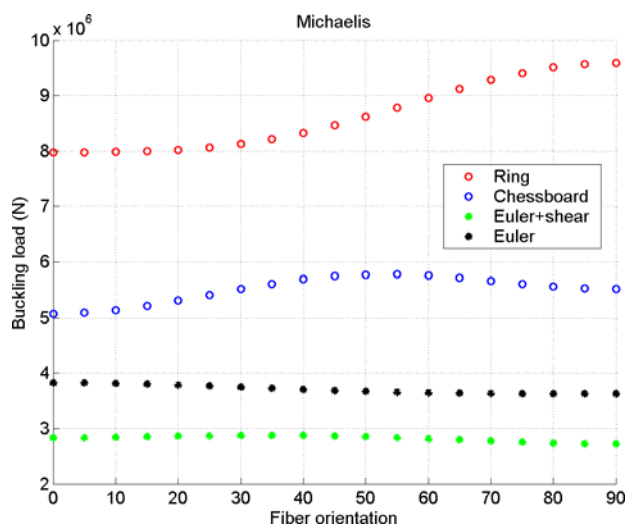


Figure 5. Influence of the cross-ply fiber orientation in the buckling mode. Wood 19mm, fiber 1mm thick. Formulation from [7]

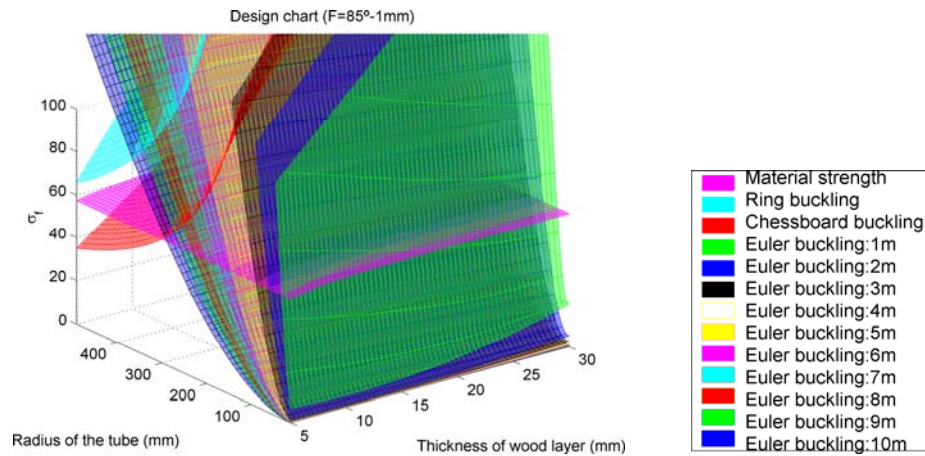


Figure 6. Three dimensional graph design for compression loading. Wood 19mm, $\pm 85^\circ$ cross-ply fiber 1mm thick.

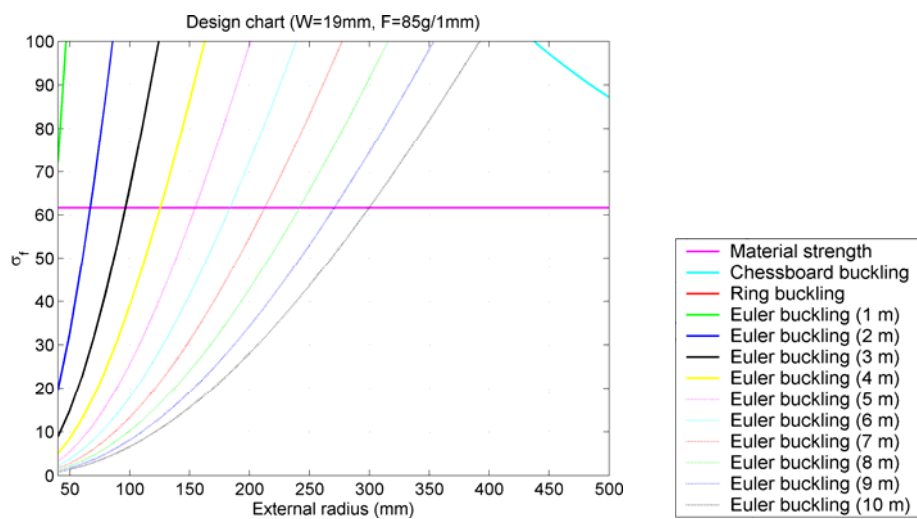


Figure 7. Bidimensional graph design for compression loading. Wood 19mm, $\pm 85^\circ$ cross-ply fiber 1mm thick

For the usual cases, the strength of the tube will be usually that of the Euler buckling or the material strength, depending on the moment of inertia of the cross section.

3.4 BIDIMENSIONAL DESIGN GRAPH

Although the previous three-dimensional graphs (Fig.6) may seem quite appealing and impressive, their reading is quite complex. A bi-dimensional graph, sectioning the previous space by determined planes may be more comprehensive for the reader. It allows for a more detailed understanding, and for a practical use.

Figure 7 shows the corresponding bi-dimensional design graph for a tube 19mm wood and $\pm 85^\circ$ fibre reinforcement 1mm thick (like those tested).

As shown, for the interval of radius depicted (up to 500mm), the failure stress never corresponds to that of the local buckling modes. The local buckling modes correspond to lower thicknesses of the wall. The failure is always that from the Euler buckling or the material strength. In the case of the tested tubes, whose radius is approximately 150mm and their length 2 500mm, the graph shows that their failure stress corresponds to that of the material. From a length of approximately 5m, the

failure would be determined by the global buckling, instead of the material.

Figure 8 shows the lines of the corresponding failure stress when varying the radius of the tube. Different series are shown, for different orientations of the fiber reinforcement. As previously, the graph is shown for a tube similar to those tested, 19mm of wood reinforced by 1mm of \pm cross-ply and 2 500mm high.

The two zones corresponding to the Euler buckling mode and to the material strength are clearly differentiated. Up to a value of approximately 75mm radius, the strength corresponds to the global Euler's buckling mode. This zone is defined by parabolic lines. From this radius, a straight line of constant value (since it is independent from the radius of the tube) marks the material strength dominated area. In the zone close to their intersection, an intermediate zone, influenced by both modes, is to be expected.

A variation in the failure values is observed in the material strength zone for the different reinforcement orientations. As previously noticed (Sect. 3.1), the highest strength corresponds to the $\pm 0^\circ$ fiber reinforcement, and the minimum to the $\pm 40^\circ$. Less variation is noticed in the area corresponding to the global buckling (as previously shown in Figure 5), but

also the highest values correspond to the $\pm 0^\circ$ reinforced

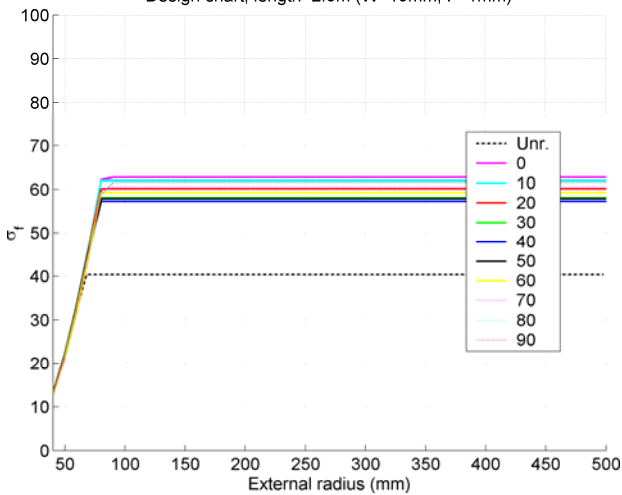


Figure 8. Graph design for compression loading for different orientations of the cross-ply fiber. Wood 19mm, cross-ply fiber 1mm thick

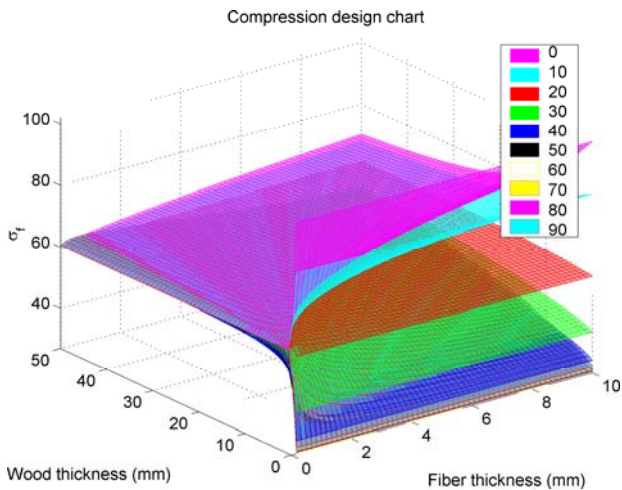


Figure 9. Modification of the failure stress in compression in relation to the thickness of wood and fiber reinforcement.

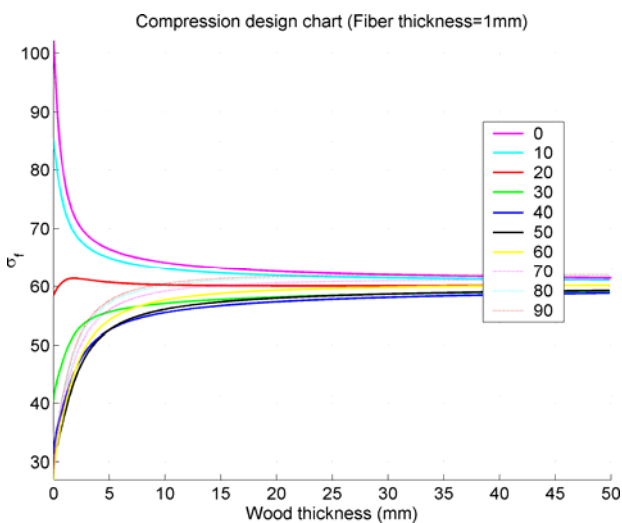


Figure 10. Modification of the failure stress in relation to the thickness of wood (cross-ply fiber thickness= 1mm).

tube, while the minimal correspond in this case to the 90° reinforced tube.

The failure response stress for the corresponding unreinforced tube is also depicted.

A clear improvement of the performance of the tube in the material controlled area is noticed. The strength of the unreinforced material is about $2/3$ of the reinforced.

However, no such difference is observed in the global buckling area. The failure stress is almost the same that the one for the reinforced tubes. One conclusion arises: for cases controlled by global buckling, reinforcing the tube does not modify its behaviour.

3.5 MATERIAL THICKNESS-FAILURE STRESS RELATION

Figure 9 shows the failure strength in relation to the wood and fiber thickness and the fiber orientation for the compression and tension loading.

As happened previously (Sect. 3.34), these three-dimensional graphs are quite difficult to read, and few conclusions may arise from them. More useful are the bi-dimensional graphs obtained by cutting these graphs by determined planes, which will be shown in the following sections. By means of the bidimensional graphs it will be possible to investigate the optimum thickness for both materials, wood (Sect 3.5.1) and fiber reinforcement (Sect. 3.5.2).

3.5.1 Wood thickness

Figure 10 shows the influence of the wood thickness in the failure stress for a compressive loading. Different series, accounting for the different orientations of the cross-ply reinforcement are also depicted.

It may be seen that, from a certain wood thickness (which may be established approximately around 25mm), the behaviour is almost constant for any of the reinforcement orientations.

The fiber reinforcements which give a better performance are initially those oriented in the direction of the load. As the thickness of the wood increases, the reinforcements perpendicular to the grain obtain better results. It can be seen how from a thickness of about 30mm, the $\pm 90^\circ$ reinforcement obtains the best performance. The perpendicular reinforcement lowers the perpendicular tension due to the Poisson effect, and this effect is higher the more wood is used. Thicker sections tend more to cracking, which is avoided by this orientation of the reinforcement.

For all the analysed range, the reinforcements around a 45° orientation give the least resistance.

When the fiber reinforcement is oriented in the direction of the load ($\pm 0^\circ$ and $\pm 10^\circ$), in the initial values of the wood thickness (from 0 to 5mm), it affects the resistance to a great extent. This initial resistance is that of the fiber, not of the wood.

For fiber angles greater than $\pm 30^\circ$, an increase in the resistance is observed until a thickness of about 15mm. From this thickness, the behaviour may be assumed as constant. An intermediate case is that of a fiber reinforcement with a $\pm 20^\circ$ orientation. In this case, a maximum is obtained for a very thin layer of wood.

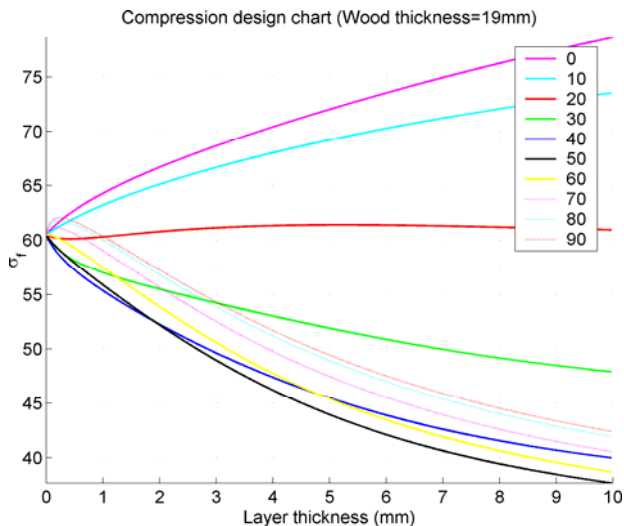


Figure 11. Modification of the failure stress in relation to the thickness of the cross-ply fiber reinforcement (wood thickness= 19mm).

It may be concluded that, for compression, an optimal use of the wood is obtained with a thickness ranging from 15 to 20mm. Higher thicknesses do not mean higher performance of the material.

3.5.2 Fiber thickness

For this analysis, the wood thickness is kept constant to a value of 19mm. This value is included in the optimum range for a compressive load, as shown in Sect. 3.5.1.

The fiber thickness depicted in the x-axis corresponds to that of a single layer of the cross-ply fiber reinforcement, which is assumed to be composed from two layers. Consequently, a value of 1mm in the graph corresponds to 2mm of the total fibre reinforcement.

Figure 11 shows the response when varying the layer thickness for a compressive load. Depending on the fiber orientation used, three different responses are observed:

- For orientations ranging from $\pm 0^\circ$ to $\pm 20^\circ$, the resistance of the composite material is directly related to that of the fiber.
- When the fiber is oriented from $\pm 30^\circ$ to $\pm 50^\circ$, the more fiber is applied to the composite material, the less strength is obtained. These orientation values also correspond to the lower resistance.
- For reinforcements between $\pm 60^\circ$ up to $\pm 90^\circ$, a maximum is located, approximately, in 0.3mm (giving, consequently, a optimal total fiber thickness of about 0.6mm). After it, their resistance quickly decreases.

It may be concluded that, for a compressive force, the optimum fiber reinforcement corresponds to an almost perpendicular orientation. But there is a point of maximum performance, for a relatively lower amount of fiber reinforcement. In the analysed case, with a wood thickness of 19mm, this was of a total reinforcement thickness of about 0.6mm.

4 CONCLUSIONS

A procedure of manufacturing wooden profiles has been developed and patented. The resulting profile encompasses efficient use of the material and optimal structural performance. An external layer of fibres is located at the outer side of the tubes, as reinforcement and protection from weathering.

The herein proposed analytical procedures have been calibrated and verified through the experimental data to assess their reliability. Predicted and experimental failure loads agreed reasonably well. Therefore, the proposed procedures are an adequate tool for the design and optimisation of wooden reinforced tubes, as shown in the parametrical analyses here presented. However, more sophisticated analytical models have to be developed and further tests on tubes with varying r/t and l/r ratios are required in the future.

ACKNOWLEDGEMENT

The Alexander von Humboldt Foundation is gratefully acknowledged for providing sponsorship to the first author. Furthermore, the authors would like to thank the German Federal Ministry of Education and Research (BMBF - Project: "High-Performance Timber Structures" Nr. 0330722A) for supporting this research.

REFERENCES

- [1] P. Haller, Concepts for textile reinforcements for timber structures, *Materials and Structures* 40 (2007) 107_118.
- [2] A. Heiduschke, J. M. Cabrero, C. Manthey, P. Haller, E. Günther, Mechanical behaviour and life cycle assessment of fibre-reinforced timber profiles, in: L. Braganca, H. Koukari, H. Blok, R. and Cervasio, M. Velkovic, R. U. V. Plewako, Z. and Landolfo, L. Silva, P. Haller (Eds.), *COST C25 Sustainability of Constructions - Integrated Approach to Lifetime Engineering*, COST C-25, European Commission, Dresden, 2008, pp. 3.38_3.46.
- [3] A. Heiduschke, P. Haller, Zum tragverhalten gewickelter formholzrohre unter axialem druck, *Bauingenieur* 84 (6) (2009) 262_269
- [4] A. Heiduschke, P. Haller. Load-carrying behavior of fiber reinforced wood profiles. *World Conference on Timber Engineering (WCTE 2010)*. June 20-24, 2010. Riva del Garda, Trentino, Italy
- [5] J.M. Cabrero. Wooden Reinforced Tubes, development of analytical and numerical models. Schriftenreihe Konstruktiver Ingenieurbau Dresden. Heft 17. ISSN 1613-6934 Dresden, 2009.
- [6] J.M. Cabrero, A. Heiduschke, P. Haller. Analytical assessment of the load carrying capacity of axially loaded wooden reinforced tubes. *Composite Structures*. Under review.
- [7] Michaeli, Walter; Huybrechts, Dirk and Wegener, Martin (1995). Dimensionieren mit Faserverbundkunststoffen: Einführung und praktische Hilfen. Hanser, München.